HHS Public Access

Author manuscript

Neurotoxicology. Author manuscript; available in PMC 2018 May 01.

Published in final edited form as:

Neurotoxicology. 2017 May ; 60: 150–160. doi:10.1016/j.neuro.2016.12.005.

Consequences of acute $Na_v1.1$ exposure to deltamethrin

T.F. James[a,b], **Miroslav N. Nenov**[a], **Cynthia M. Tapia**[a], **Marzia Lecchi**[c], **Shyny Koshy**[a,f], **Thomas A. Green**[a,f], and **Fernanda Laezza**[a,d,e,f,*]

[a] Department of Pharmacology & Toxicology, University of Texas Medical Branch, USA

[b] Neuroscience Graduate Program, University of Texas Medical Branch, USA

[c] Department of Biotechnology and Bioscience, University of Milano-Bicocca, Italy

[d] Mitchell Center for Neurodegenerative Diseases, USA

[e] Center for Environmental Toxicology, University of Texas Medical Branch, USA

[f] Center for Addiction Research, University of Texas Medical Branch, USA

Abstract

Background—Pyrethroid insecticides are the most popular class of insecticides in the world, despite their near-ubiquity, their effects of delaying the onset of inactivation of voltage-gated sodium (Na_v) channels have not been well-evaluated in all the mammalian Na_v isoforms.

Objective—Here we compare the well-studied $Na_v1.6$ isoforms to the less-understood $Na_v1.1$ in their responses to acute deltamethrin exposure.

Methods—We used patch-clamp electrophysiology to record sodium currents encoded by either $Na_v1.1$ or $Na_v1.6$ channels stably expressed in HEK293 cells. Protocols evaluating both resting and use-dependent modification were employed.

Results—We found that exposure of both isoforms to 10 μM deltamethrin significantly potentiated persistent and tail current densities without affecting peak transient current densities, and only $Na_v1.1$ maintained these significant effects at 1 μM deltamethrin. Window currents increased for both as well, and while only $Na_v1.6$ displayed changes in activation slope and $V_{1/2}$ of steady-state inactivation for peak currents, $V_{1/2}$ of persistent current activation was hyperpolarized of ~10 mV by deltamethrin in $Na_v1.1$ cells. Evaluating use-dependence, we found that deltamethrin again potentiated persistent and tail current densities in both isoforms, but only $Na_v1.6$ demonstrated use-dependent enhancement, indicating the primary deltamethrin-induced effects on $Na_v1.1$ channels are not use-dependent.

Conclusion—Collectively, these data provide evidence that $Na_v1.1$ is indeed vulnerable to deltamethrin modification at lower concentrations than $Na_v1.6$, and this effect is primarily mediated during the resting state.

* Corresponding author at: Department of Pharmacology & Toxicology, Center for Addiction Research, Center for Biomedical Engineering and Mitchell Center for Neurodegenerative Diseases, University of Texas Medical Branch, 301 University Boulevard, Galveston, TX, 77555, USA. felaezza@utmb.edu (F. Laezza).

Conflict of interest

None.

General significance—These findings identify $Na_v1.1$ as a novel target of pyrethroid exposure, which has major implications for the etiology of neuropsychiatric disorders associated with loss of $Na_v1.1$-expressing inhibitory neurons.

1. Introduction

Pyrethroids are a class of insecticides analogous to the natural pyrethrins found in the chrysanthemum family (Tan and Soderlund, 2010; Breckenridge et al., 2009). Safer than their organo-phosphate predecessors, pyrethroids have become the most popular class of insecticides over the past three decades, with use increasing each year as organophosphate use decreases (Power and Sudakin, 2007). In 2013, pyrethroids accounted for the largest category (over 25%) of single substance, non-pharmaceutical exposure cases in the United States (Mowry et al., 2014). Pyrethroids are also readily available to the general public in the form of household insecticidal sprays. Such widespread, unregulated use increases exposure and development of adverse disorders, with new evidence documenting pyrethroid bioaccumulation (Corcellas et al., 2015) and pyrethroid correlations with adverse neuronal outcomes (Oulhote and Bouchard, 2013; Viel et al., 2015; Richardson et al., 2015). Alarming evidence from recent large-scale epidemiological studies identifies early life exposure to deltamethrin as a risk factor for autism spectrum disorders and cognitive impairment raising the need for further investigation of its neurotoxicity in the developing brain (Viel et al., 2015).

Pyrethroids exert their insecticidal effects by delaying the onset of inactivation in voltage-gated sodium (Na_v) channels, which disrupts electrical communication (Ray and Fry, 2006; Chinn and Narahashi, 1986; Motomura and Narahashi, 2001). Na_v channels are similarly the target of neurotoxic effects in mammals but are accompanied with a wider array of responses due to Na_v isoform diversity in mammals (Tan and Soderlund, 2010, 2009; He and Soderlund, 2011; McCavera and Soderlund, 2012). Na_v channels in the mammalian brain are comprised of a functional, pore-forming α subunit with accessory β subunits (Goldin, 2001; Catterall, 2000). The α subunit has 9 mammalian isoforms ($Na_v1.1$–$Na_v1.9$), each with distinct pharmacological and functional properties and varied distribution in excitable cells (Catterall et al., 2005; Cusdin et al., 2008; Shavkunov et al., 2013; Ogiwara et al., 2007). Four of the nine isoforms are strongly expressed in the mammalian brain— $Na_v1.1$, $Na_v1.2$, $Na_v1.3$, and $Na_v1.6$ (He and Soderlund, 2011; Catterall et al., 2005; Shavkunov et al., 2013; James et al., 2015; Leterrier et al., 2010). Each α subunit is composed of four homologous domains with six transmembrane segments in each (Catterall, 2000; Catterall et al., 2005; O'Reilly et al., 2006). Several residues critical for conferring pyrethroid sensitivity or resistance have been found in the IS6, IIS6, and IIIS6 segments, the IIS5 segment, and the IIS4-IIS5 linker region (O'Reilly et al., 2006; Oliveira et al., 2013; Tan et al., 2005), regions which are known to be involved in the inactivation of Na_v channels (Catterall et al., 2005; Yarov-Yarovoy et al., 2001, 2002).

Pyrethroids are divided into two categories based on structure— Type I pyrethroids lack the α-cyano functional group found in the Type II category (Breckenridge et al., 2009). Type I pyrethroid acute exposures are correlated with a T syndrome characterized by tremors while type II pyrethroid acute exposures correlate with a CS syndrome characterized by

choreoathetosis with salivation (Breckenridge et al., 2009; Romero et al., 2015). Furthermore, type I pyrethroids have a higher propensity for resting-state modification of Na_v channels whereas type II pyrethroids have a higher affinity for the open state of a Na_v channel (Tan and Soderlund, 2010; Breckenridge et al., 2009; He and Soderlund, 2011; McCavera and Soderlund, 2012). These correlations are strong but not absolute, as some pyrethroids demonstrate activity associated with both categories of pyrethroid action (Tan and Soderlund, 2010; Breckenridge et al., 2009; He and Soderlund, 2011). Deltamethrin is one example of a pyrethroid that can have both type I and type II activity. One of the more potent pyrethroids, deltamethrin contains an α-cyano group and has very strong activity associated with type II pyrethroids but simultaneously demonstrates some effects associated with type I pyrethroids (Tan and Soderlund, 2010; Breckenridge et al., 2009).

Previous studies have demonstrated that $Na_v1.6$ is sensitive to pyrethroid activity while other isoforms like $Na_v1.2$ are more resistant but not impervious (Tan and Soderlund, 2010; He and Soderlund, 2011; McCavera and Soderlund, 2012; O'Reilly et al., 2006; Oliveira et al., 2013; Tan et al., 2005). The V409 residue in cockroach sodium channel is involved on conferring natural sensitivity to pyrethroid activity, and when this residue is mutated to an isoleucine, pyrethroid resistance occurs (Oliveira et al., 2013). The valine residue is conserved in human $Na_v1.6$ but is replaced by isoleucine in both $Na_v1.1$ and $Na_v1.2$ (Oliveira et al., 2013). As $Na_v1.2$ and $Na_v1.1$ are phylogenetically closely related (Goldin, 2001; Catterall et al., 2005), the presence of isoleucine at the cockroach 409 position in both isoforms suggests both channels may behave similarly to an acute pyrethroid exposure. As the primary Na_v channel isoform expressed in fast-spiking GABAergic interneurons in the brain, $Na_v1.1$ plays an essential role in synchronizing brain activity during cognitive tasks which are disrupted in neurodevelopmental disorders, such as autism and schizophrenia (Berkowicz et al., 2016; Dong et al., 2016; Inan et al., 2016; Jiang et al., 2013; McNally et al., 2013). On this premise we have hypothesized that the detrimental effects of early life exposure to deltamethrin might be reconciled with its brain toxicity for $Na_v1.1$ channels. To test this hypothesis, we studied the pharmacological activity of deltamethrin in $Na_v1.1$ channels expressed in heterologous cell systems using the well-studied $Na_v1.6$ as a comparative reference.

Here we present the action of deltamethrin on human $Na_v1.1$ or $Na_v1.6$ channels stably expressed in HEK293 cells. Our results show that deltamethrin induces significant modification of $Na_v1.1$ persistent and tail currents in its resting state with little reliance on channel opening to exert its effect. Compared with the better-studied $Na_v1.6$, deltamethrin induced significant changes to persistent and tail currents that occur at lower concentrations in $Na_v1.1$ than in $Na_v1.6$. These findings suggest that $Na_v1.1$ is susceptible to deltamethrin modification, more amenable to modification at resting states, and sensitive to deltamethrin at lower concentrations than $Na_v1.6$, identifying $Na_v1.1$ as the preferential associative link to increased risk for neuropsychiatric disorders and early-life exposure to deltamethrin.

2. Materials and methods

2.1. Chemicals

Deltamethrin was dissolved in DMSO (Sigma, St. Louis, MO) to a stock concentration of 100 mM, aliquoted, and stored at −20 ° C for further use. Aliquots were then removed the day of experimentation, thawed, and added to the bath solution to make a final concentration of 0.01% DMSO and 10 μM deltamethrin if present. Deltamethrin was diluted further to 1 and 0.1 μM when mentioned, and DMSO controls were adjusted to 0.001% and 0.0001% final solution.

2.2. Cell culture

All reagents were purchased from Sigma-Aldrich (St. Louis, MO) unless noted otherwise. HEK-293 cells stably expressing either human $Na_v1.6$ or human $Na_v1.1$ (gifts from Drs. Marzia Lecchi and Enzo Wanke, Università degli Studi di Milano-Bicocca, Milano, Italy) were maintained in medium composed of equal volumes of DMEM and F12 (Invitrogen, Carlsbad, CA) supplemented with 0.05% glucose, 0.5 mM pyruvate, 10% fetal bovine serum, 100 U/ml penicillin, 100 μg/mL streptomycin, and 500 μg/mL G418 (Invitrogen) for selection of stably transfected cells, and incubated at 37 ° C with 5% CO_2, as previously described (Shavkunov et al., 2013). The human Nav 1.6 and human Nav 1.1 HEK cell lines were validated through RT-PCR using the following primers specific to the particular human isoform: Nav1.1Fw TCTCTTGCGGCTATTGAAAGAC, Nav1.1Rv GGGCCATTTTCGTCGTCATCT, Nav1.6Fw CCTTTCACCCCTGAGTCACTG, Nav1.6Rv AGGTCGCTGTTTGGCTTGG.

2.3. Electrophysiology

HEK-293 cells stably expressing either human $Na_v1.1$ or human $Na_v1.6$ were dissociated and re-plated at low-density. Recordings were performed at room temperature (20–22 ° C) using an Axopatch 200B amplifier (Molecular Devices, Sunnyvale, CA), and deltamethrin (10 μM, ABCam, Cambridge, MA) or DMSO (0.01% maximum final concentration, Sigma, St. Louis, MO) were added to the bath solution prior to transfer. Where mentioned, concentrations of 1 and 0.1 μM were used along with appropriate DMSO controls (0.001% and 0.0001% final concentration, respectively). Cells were allowed to rest in solution, exposed to the drug or vehicle, for approximately 30 min before beginning experiments. Recording continued after this period for one hour, resulting in 1.5 h of exposure to drugs. Borosilicate glass pipettes with resistances of 3–8 MΩ were made using a Narishige PP-83 vertical Micropipette Puller (Narishige International Inc., East Meadow, NY). The recording solutions were as follows: extracellular (mM): 140 NaCl, 3 KCl, 1 $MgCl_2$, 1 $CaCl_2$, 10 HEPES, 10 glucose, pH 7.3; intracellular: 130 CH_3O_3SCs, 1 EGTA, 10 NaCl, 10 HEPES, pH 7.3. Membrane capacitance and series resistance were estimated by the dial settings on the amplifier. Individual membrane capacitance (~9 pF average) was used to calculate current density, which allows for comparison with cells of all sizes, and cells exhibiting a series resistance of 25 MΩ or higher were excluded from analysis. Capacitive transients and series resistances were compensated electronically by 70–80%. Data were acquired at 20 kHz and filtered at 5 kHz prior to digitization and storage. All experimental parameters were controlled by Clampex 9 software (Molecular Devices) and interfaced to the

electrophysiological equipment using a Digidata 1200 analog–digital interface (Molecular Devices). Voltage-dependent inward currents were evoked by depolarizations to test potentials between −60 mV and +70 mV from a holding potential of −70 mV. Steady-state (fast) inactivation of Na_v channels was measured with a paired-pulse protocol. From the holding potential, cells were stepped to varying test potentials between −110 mV and 20 mV (prepulse) prior to a test pulse to −10 mV. Use-dependence was determined with a depolarization to −10 mV followed by a train of sub-threshold depolarizations to −30 mV at 10 Hz or 5 Hz frequency that terminates in another, final test pulse to −10 mV; this protocol was adapted from Dong and Priestley (2003) to assess use-dependence in absence of a continuous perfusion system, as traditional use-dependence protocols used for pyrethroid research did not fit with our current experimental model.

2.4. Electrophysiology data analysis

Current densities were obtained by dividing Na^+ current (I_{Na}) amplitude by membrane capacitance. Current–voltage relationships were generated by plotting current density as a function of the holding potential. Conductance (G_{Na}) is calculated by the following Eq. (1):

$$G_{Na} = \frac{I_{Na}}{(V_m - E_{rev})} \quad (1)$$

where I_{Na} is the current amplitude at voltage V_m, and E_{rev} is the Na^+ reversal potential.

Steady-state activation curves were derived by plotting normalized G_{Na} as a function of test potential and fitted using the Boltzmann Eq. (2):

$$\frac{G_{Na}}{G_{Na,Max}} = 1+e^{\left[\frac{(V_a-E_m)}{k}\right]} \quad (2)$$

where $G_{Na,Max}$ is the maximum conductance, V_a is the membrane potential of half-maximal activation, E_m is the membrane voltage and k is the slope factor. For steady-state inactivation, normalized current amplitude ($I_{Na}/I_{Na,Max}$) at the test potential was plotted as a function of prepulse potential (V_m) and fitted using the Boltzmann Eq. (3):

$$\frac{I_{Na}}{I_{Na,Max}} = \frac{1}{\left\{1+e^{\frac{V_h-E_m}{k}}\right\}} \quad (3)$$

where V_h is the potential of half-maximal inactivation and k is the slope factor. The percent of deltamethrin-modified channels were calculated using methods and equations as outlined in (Tatebayashi and Narahashi, 1994) and fit to the Hill equation. Use-dependent peak current densities were taken from the final test pulse of the use-dependent protocol. Persistent, use-dependent current densities are taken as the mean current remaining after the transient current has ended and reached steady-state, again derived from the final test pulse.

Tail currents are defined as the current that passes through remaining, opened Na_v channels approximately 0.5 ms after termination of the depolarizing signal. Expressing tail currents over peak currents from the same depolarizing signal is termed the fraction of available current. Total charge was calculated by integrating the current signal after termination of the final test pulse and before the return to resting membrane potential. All modification values are calculated by expressing final test pulse values over the initial test pulse values. Data analysis was performed using Clampfit 9 software (Molecular Devices, USA) and Origin 8.6 software (OriginLab, Northampton, MA, USA).

2.5. Statistical analysis

Deltamethrin-induced effects were quantified and compared to DMSO controls for both isoforms. After testing for normality, a Student's *t*-test or a Mann-Whitney *U* test was used to make comparisons for parametric and non-parametric data, respectively. Statistical tests were performed with Origin 8.6 software (Origin-Lab, Northampton, MA, USA) and verified with SigmaPlot (Systat Software Inc., San Jose, CA, USA).

3. Results

3.1. Effects of deltamethrin on evoked properties

3.1.1. Effects of deltamethrin on peak transient current densities—We applied whole-cell patch-clamp electrophysiology to explore the action of deltamethrin on human $Na_v1.1$ or $Na_v1.6$ channels stably expressed in HEK293 cells. To assess the ability of deltamethrin to affect the resting state of Na_v channels, we allowed HEK-Na_v cells to rest in bath solution treated with one of three concentrations of DMSO (0.01, 0.001, or 0.0001% final concentration) or deltamethrin (10, 1, or 0.1 μM) for at least 30 min. A standard step-wise protocol was used to assess evoked properties after 30 min of bath incubation with drug, and representative traces of both protocol and results are depicted in Fig. 1A and B. Illustrated in Fig. 1, deltamethrin did not significantly affect the peak transient current densities evoked at −10 mV in $Na_v1.1$ cells during a depolarizing pulse (167.5 ± 42.1 pA/pF, n = 14) relative to control values (115.0 ± 37.2 pA/pF, n = 9, p = 0.27, Fig. 1C) at the highest concentration of deltamethrin. Similarly, $Na_v1.6$ control cells did not display a significant alteration of peak transient current densities at −10 mv (56.1 ±12.6 pA/pF, n = 10) when treated with 10 μM deltamethrin (29.3 ± 4.4 pA/pF, n = 20, p = 0.09, Fig. 1D).

3.1.2. Effects of deltamethrin on window currents—Fitted curves of the voltage-dependence of activation (derived from protocols illustrated Fig. 1A and B) and steady-state inactivation, ascertained using a two-step protocol, are displayed in Fig. 1. $Na_v1.1$ DMSO control cells exhibited a $V_{1/2}$ of activation of −22.6 ± 2.7 mV (n = 7) with a slope factor of 2.9 ± 0.42. Delta-methrin did not produce a significant change of $V_{1/2}$ of activation (−27.2 ± 6.7 mV, n = 12, p = 0.18, Fig. 1E) or the slope factor (3.9 ± 0.60, p = 0.30). $Na_v1.6$ cells also did not show a significant alteration of $V_{1/2}$ of activation in DMSO control cells (−20.7 ± 1.3 mV, n = 10) compared with deltamethrin cells (−23.8 ± 1.3 mV, n = 17, p = 0.14, Fig. 1F). $Na_v1.6$ cells did, however, display a significantly altered slope factor between control cells (3.6 ± 0.3, n = 10) and deltamethrin cells (5.0 ± 0.3, n = 17, p = 0.01). $Na_v1.1$ DMSO control cells exhibited a $V_{1/2}$ of steady-state inactivation of −50.4 ± 5.0 (n = 8) with an

accompanying slope factor of 5.9 ± 0.7. Deltamethrin did not produce a significant change in neither $V_{1/2}$ of steady-state inactivation (−53.9 ± 4.7, n = 13, p = 0.12, Fig. 1E) nor the slope factor (5.2 ± 0.4, p = 0.75). $Na_v1.6$ channels did show a significant shift in the voltage-dependence of steady-state inactivation with control cells demonstrating a $V_{1/2}$ of −56.6 ± 0.8 mV (n = 12) that was hyperpolarized to −64.5 ± 1.3 mV (n = 15, p < 0.001, Fig. 1F). This alteration was not accompanied with a change in slope factor, as DMSO cells exhibited a k value of 5.9 ± 0.2 (n = 12) that was not statistically different from the deltamethrin average of 5.8 ± 0.3 (n = 15, p = 0.15). Activation and inactivation curves are superimposed in Fig. 1E and F in order to demonstrate the window currents (shaded regions) of each isoform with or without deltamethrin. Deltamethrin induces large increases to window currents in both isoforms, but the magnitude is larger in $Na_v1.1$. Furthermore, the isoforms demonstrate visually distinct shapes of their window currents, especially with respect to the inactivation curve. These data suggest that deltamethrin does not have a significant impact on the $V_{1/2}$ of activation or steady-state inactivation of peak transient currents in $Na_v1.1$ but does have a profound impact on the $V_{1/2}$ of persistent current activation. The same is not true for $Na_v1.6$, as deltamethrin induces significant alterations of steady-state inactivation in addition to generation of a persistent current. Visual inspection of window currents, however, reveals that deltamethrin has a profound effect on the channel opening in both isoforms, but such effects may vary between isoforms.

3.1.3. Effects of deltamethrin on persistent and tail current densities—Persistent and tail currents of both isoforms were studied using the same protocols shown in Fig. 1, but with variable concentrations of deltamethrin and corresponding DMSO control. Derived from the same protocols portrayed in Fig. 1, representative traces in Fig. 2A and B show persistent currents that remain after the fast transient has inactivated along with tail currents shown in the inset. In this study, persistent current is defined as the mean current over 20 ms measured 10 ms before the termination of the depolarizing potential. With this definition, 10 μM deltamethrin produced a significant potentiation of the persistent $Na_v1.1$ current densities (53.6 ± 9.5 pA/pF, n = 12) in relation to DMSO control values (10.2 ± 5.4, n = 4, p = 0.03, Fig. 2C) at −20 mV. In a similar fashion, at −20 mV, $Na_v1.6$-encoded persistent current densities were also increased from DMSO control (−0.4 ± 0.6 pA/pF, n = 6) with 10 μM deltamethrin application (9.2 ± 2.4 pA/pF, n = 20, p < 0.01, Fig. 2D). However, 1 μM deltamethrin maintains a significant potentiation of persistent current density exclusively in $Na_v1.1$ from −2.7 pA/pF (n = 3) in DMSO control cells to 17.6 pA/pF (n = 20, p = 0.02, Fig. 2C) with deltamethrin. $Na_v1.6$ persistent current densities are not significantly altered by deltamethrin at a 1 μM concentration (Fig. 2D). Further parameters are summarized in Table 1. Both $Na_v1.1$ and $Na_v1.6$ cells treated with deltamethrin displayed a persistent current. However, not all DMSO cells displayed persistent current, and those were excluded in the comparison. Tail current densities increased with voltage in DMSO control cells in a relatively linear fashion, but the slope of the voltage-dependency of the $Na_v1.1$ tail currents, derived from the I–V curve (Fig. 2C and E) are significantly altered with deltamethrin treatment at both 10 and 1 μM. While DMSO control cells' tail current densities steadily increased to peak at maximum positive voltage, deltamethrin-treated $Na_v1.1$ cells displayed a shifted peak that occurred at −10 mV and was followed with slight attenuation at higher voltages (Fig. 2E) in the two higher concentrations. $Na_v1.6$ cells did not mirror the slope

effect observed in $Na_v1.1$ cells at any concentration. Taken at the observed peak of −10 mV in $Na_v1.1$ cells, DMSO control cells exhibited a tail current density of 21.4 ± 6.3 pA/pF (n = 9) that was significantly increased to 114.8 ± 17.9 pA/pF (n = 14, $p < 0.001$, Fig. 2E) with deltamethrin treatment. $Na_v1.6$ also demonstrated significant potentiation of tail currents from 5.9 ± 1.5 pA/pF (n = 10) in DMSO control cells to 25.1 ± 4.1 pA/pF (n = 20, $p < 0.001$, Fig. 2F) with 10 μM deltamethrin At 0.01% DMSO, $Na_v1.1$ control cells exhibited a tail current density of 1.2 pA/pF (n = 3) that was potentiated to 77.8 pA/pF (n = 9, $p = 0.04$) with 1 μM deltamethrin, and this potentiation was not observed in $Na_v1.6$ cells with the same concentration of deltamethrin (Fig. 2E and F). It was found that DMSO has a slight effect on current densities in $Na_v1.1$, and therefore we could not generate a canonical dose-response curve. These data indicate that deltamethrin does not have a major impact on transient current densities in either isoforms, but it does have a sizeable effect on persistent and tail current magnitudes and tail current shape in both isoforms at 10 μM. Reducing this concentration to 1 mM abolished significant effects in $Na_v1.6$ but not in $Na_v1.1$; however, all significant effects do disappear at 0.1 μM deltamethrin (Fig. 2C–F). These data suggest that while deltamethrin has profound effects on both $Na_v1.1$ and $Na_v1.6$ in the resting state, and that $Na_v1.1$ is more sensitive to resting-state modification carried out by deltamethrin at lower concentrations than $Na_v1.6$.

Applying the same method used for peak current densities to persistent current densities, the voltage-dependence of persistent current was also determined. In $Na_v1.1$ cells, a robust and significant hyperpolarizing shift was detected in the $V_{1/2}$ of persistent current activation of deltamethrin cells (−34.7 ± 1.1 mV, n = 16, $p < 0.001$, Table 1) compared to DMSO control cells (−22.8 ± 1.4 mV, n = 4). Changes to $V_{1/2}$ were also reflected in the slope factor for $Na_v1.1$ cells, as the DMSO average slope factor was 6.5 ± 0.9 (n = 4) and changed to 2.8 ± 0.3 (n = 16, $p < 0.001$) in deltamethrin cells. In $Na_v1.6$ cells, no DMSO control cells exhibited persistent currents with a sigmoidal voltage relationship, and therefore we could not generate an activation curve for this group. Deltamethrin-treated $Na_v1.6$ cells did show a $V_{1/2}$ of activation of persistent current of −26.8 ± 1.4 mV (n = 9, data not shown). Additional analysis performed by normalizing persistent sodium currents to DMSO transient peak currents (Fig. 3A and B) revealed that deltamethrin had a stronger effect on Nav1.1 than Nav1.6 (at voltage step −10 mV–57.4 ± 8.8% in Nav1.1 cells, n = 17 versus 14.5 ± 4.2% in Nav1.6 cell, n = 20; $p < 0.0005$ with Student *t*-test).

Finally, the maximum percentage of deltamethrin-modified channels (M_{max}) and K_d values were calculated using equation from (Tatebayashi and Narahashi, 1994) and fitting with Hill equation, respectively (Fig. 3C). At 10 μM of deltamethrin M_{max} was 56.05 ± 5.7% for Nav1.1 (n = 19) versus 33.4 ± 4.4% for Nav1.6 (n = 14), a difference that was statistically significant ($p < 0.005$ with Student, *t*-test). Differences in M_{max} from the two isoforms were mirrored by K_d (0.49 μM for Nav1.1 versus 0.92 μM for Nav1.6), reinforcing the notion that $Na_v1.1$ channels are more susceptible to deltamethrin modification than Nav1.6

3.2. Effects of deltamethrin on use-dependent properties

Previous research has established that deltamethrin has high affinity for the open (active) state of Na_v channels (He and Soderlund, 2011; McCavera and Soderlund, 2012; Dong and

Priestley, 2003), and we therefore tested this aspect of function as well. Use-dependent activity of deltamethrin was assessed with two separate test pulses to −10 mV prior to or after a train of sub-threshold depolarizations to −30 mV at a rate of 10 or 5 Hz, and representative traces of the protocols and their results are shown in Fig. 4. No major differences were observed between stimulation frequency groups, therefore, henceforth, all values mentioned in this text will refer to the 5 Hz protocol. All values are summarized in Table 2 and illustrated in Fig. 4. For $Na_v1.1$, control cells displayed a peak transient current density of 101.6 ± 26.6 pA/pF (n = 10, Fig. 4D), and expression of this value over the value obtained from the initial test pulse indicates that these cells demonstrate a 101.6 ± 2.8% alteration of use-dependent, peak, transient current densities (Fig. 4F). Deltamethrin-exposed cells displayed a final peak current density of 121.8 ± 24.2 pA/pF (n = 17) that was not significantly different from DMSO control (Fig. 4D). This value was a 99.9 ± 4.4% change from initial test values, which is not significantly different from DMSO control (Fig. 4F). In $Na_v1.6$ cells, DMSO control cells exhibited a peak current density of 42.1 ±12.5 pA/pF (n = 11) while deltamethrin peak, transient current densities were 25.5 ± 4.3 pA/pF (n = 19), which was not a statistically significant change (Fig. 4D). However, $Na_v1.6$ cells did show a significant ability to undergo use-dependent change, as DMSO cells displayed current densities that are 96.5 ± 2.4 (n = 11) while deltamethrin-treated cells displayed a 120.6 ± 8.0% (n = 19, $p < 0.001$) increase from their initial values (Fig. 4F). These data indicate that neither Na_v channel isoform displays a use-dependent effect on peak current densities relative to DMSO controls, but $Na_v1.6$ does display a significant use-dependent potentiation of peak current densities after a train of depolarizing potentials.

Applying the same definition outlined in Section 3.1.2 to the use-dependent test pulses in our protocol, $Na_v1.1$ DMSO control cells displayed small degrees of persistent current densities of −1.1 ± 2.0 pA/pF (n = 10) that represent a 67.4 ± 27.4% alteration of initial values. Deltamethrin significantly potentiated persistent current to 60.5 ± 7.6 pA/pF (n = 17, $p < 0.001$, Fig. 4H), but the degree of this alteration was not significantly different at 83.6 ± 10.7% (Fig. 4J). For $Na_v1.6$, persistent current densities were −3.5 ± 1.8 pA/pF (n = 12) in DMSO control cells, and deltamethrin application significantly potentiated the persistent current to 11.8 ± 2.5 pA/pF (n = 19, $p < 0.001$, Fig. 4H). In DMSO cells, the final persistent currents were 136.7 ± 36.0% (n = 11) of their initial values while deltamethrin cells exhibited a significantly larger increase in persistent current at 253.8 ± 50.8% (n = 18, p = 0.01, Fig. 4J) of the initial values. These data suggest that while deltamethrin induces substantial and significant persistent current in both Na_v isoforms, only $Na_v1.6$ demonstrates reliance upon channel use in order to exert or enhance its effect. This observation may indicate that $Na_v1.1$ is more heavily modified by deltamethrin during its resting state than $Na_v1.6$.

Deltamethrin affected tail currents in a similar fashion. $Na_v1.1$ DMSO control cells displayed a tail current density of 17.9 ± 3.4 pA/pF (n = 10) which was a 107.7 ± 4.4% change from initial test pulse values. These densities were significantly potentiated to 147.8 ± 18.1 (n = 17, $p < 0.001$, Fig. 4E) with deltamethrin treatment, and this potentiation represented a 127.1 ± 9.8% (n = 17, Fig. 4G) change from initial values, which was not statistically significant. $Na_v1.6$ DMSO controls cells displayed tail current densities of 14.3 ± 3.6 pA/pF (n = 12) while deltamethrin-treated cells exhibited tail current densities of 45.5

± 5.7 pA/pF (n = 20, $p < 0.001$, Fig. 4E) that were significantly larger. Furthermore, the DMSO-exposed cells demonstrated a 107.8 ± 4.6% (n = 12) change from initial values, and deltamethrin treatment lead to a significantly larger degree of change of 131.0 ± 5.1% (n = 20, $p < 0.001$, Fig. 4G). Expressing tail current densities over their paired transient peak current density was used as a measure of inactivation-resistant Na_v channels and was termed *fraction of available current*. $Na_v1.1$ control cells displayed a fraction of available current of 0.27 ± 0.06 (n = 9), and deltamethrin treatment significantly increased this fraction to 1.49 ± 0.16 (n = 17 Fig. 4I). Similarly, $Na_v1.6$ control cells exhibited a fraction of available current of 0.10 ± 0.28 (n = 11) that was significantly increased in cells treated with deltamethrin to 2.12 ± 0.26 (n = 19, $p < 0.01$, Fig. 4I). Collectively, these data indicate that deltamethrin significantly increases the inactivation resistance of both Na_v isoforms; however, significant and use-dependent changes occur exclusively in $Na_v1.6$ whereas any significant effects created by deltamethrin application to $Na_v1.1$ channels likely occurred during rest and not during channel opening.

Because of the high persistence of the sodium current induced by deltamethrin, we were unable to determine the time-constant of decay of the tail currents and therefore measured total flux. $Na_v1.1$ control cells exhibited a total flux of 1087.4 ± 389.2 nC (n = 10), and deltamethrin treatment significantly increased this total flux to 28143.5 ± 3745.8 nC (n = 17, $p < 0.001$, Fig. 4K). For $Na_v1.6$, DMSO cells displayed a total charge of 747.3 ± 218.5 nC (n = 12) that was significantly increased to 6080.3 ± 805.0 nC (n = 20, $p < 0.001$, Fig. 4K). Deltamethrin treatment significantly potentiated the amount of charge flux for each isoform, yet its effect on $Na_v1.1$ channels is larger than $Na_v1.6$. These observations suggest that while deltamethrin exerts more use-dependent changes on $Na_v1.6$ than $Na_v1.1$, its effect on the latter is still profound.

4. Discussion

This study represents the first description of deltamethrin action on the $Na_v1.1$ α subunit isoform stably expressed in HEK293 cells. We acknowledge that our use of a subunits without accompanying β subunits may not be reflective of several native mammalian Na_v channel (Hartshorne and Catterall, 1984; Wildburger et al., 2015). Nevertheless, knowledge of naked a subunit behavior will inform future studies of Na_v channels expressed with β subunits. Past studies have postulated that the residue corresponding to V409 in cockroach sodium channel is critical for conferring pyrethroid resistance or susceptibility (O'Reilly et al., 2006; Oliveira et al., 2013; Tan et al., 2005; Du et al., 2011; Vais et al., 2000). In the $Na_v1.2$ isoform, it is believed that an isoleucine at this position renders the channel more resistant to pyrethroid modification (O'Reilly et al., 2006; Oliveira et al., 2013), and the presence of valine at this position in the $Na_v1.6$ isoform is critical for relatively increased susceptibility to pyrethroids compared to $Na_v1.2$ (O'Reilly et al., 2006; Oliveira et al., 2013; Tan et al., 2005; Du et al., 2011; Vais et al., 2000). We found that deltamethrin did not produce a significant change in peak current densities of neither $Na_v1.1$ nor $Na_v1.6$ α subunits expressed in HEK293 cells. These findings are consistent with similar results with other Na_v isoforms in which pyrethroids alter the ability of a Na_v channel to inactivate without affecting peak current densities (Tan and Soderlund, 2010, 2009; Chinn and Narahashi, 1986; He and Soderlund, 2011; McCavera and Soderlund, 2012). We found that

deltamethrin did not significantly influence voltage dependence of activation for either isoform; however, a significant shift in slope was detected only for $Na_v1.6$. An approximately 8 mV hyperpolarizing shift in the voltage-dependence of steady-state inactivation was detected only in $Na_v1.6$ with no significant change to slope. For $Na_v1.1$, values for $V_{1/2}$ of activation and steady-state inactivation are consistent with established values of $Na_v1.1$ in HEK293 cells (Qiao et al., 2014) with minor differences attributable to varied culture protocols, reagents, and our use of DMSO as a control. Deltamethrin did not produce a significant change in the $V_{1/2}$ for activation, which is not consistent with previous studies demonstrating that deltamethrin hyperpolarizes the $V_{1/2}$ for both activation and steady-state inactivation (Tan and Soderlund, 2010, 2009; He and Soderlund, 2011). Our values and outcomes for these parameters in $Na_v1.6$ differ somewhat from other studies' findings (Tan and Soderlund, 2010; He and Soderlund, 2011; McCavera and Soderlund, 2012), a disparity that might be attributed to species differences. Compared with HEK293 cells prepared similarly to ours with expression of rat $Na_v1.6$, our human $Na_v1.6$ appears to be less sensitive to deltamethrin modification than the rat $Na_v1.6$ used in the same HEK293 expression system (He and Soderlund, 2015). Without varying methods of expression, it is then likely that the differences seen between rat and human $Na_v1.6$ stem from differences between the two species. Inter-species differences in pyrethroid sensitivity have been demonstrated before for Nav1.3 (Tan and Soderlund, 2009), thus it is important to consider that rodent models of deltamethrin activity may not sufficiently represent what occurs in humans. Inspection of window currents suggests that $Na_v1.1$ is still affected by deltamethrin application, but these changes may not best be reflected by peak currents. In this context, $Na_v1.6$ peak current densities are more sensitive to deltamethrin modification.

Both $Na_v1.1$ and $Na_v1.6$ persistent current densities were significantly potentiated with 10 μM deltamethrin, but only $Na_v1.1$ demonstrated significant potentiation when deltamethrin was reduced to 1 μM. These findings are consistent with previous studies indicating that deltamethrin has a potent impact on persistent (or "late") currents in $Na_v1.6$ channels (Tan and Soderlund, 2010; He and Soderlund, 2011, 2015). It was, however, surprising to find that a lower deltamethrin concentration was sufficient to effect significant change in $Na_v1.1$ and not $Na_v1.6$, which was not predicted based on comparisons with other isoforms (Catterall et al., 2005; O'Reilly et al., 2006; Oliveira et al., 2013; Tan et al., 2005; Du et al., 2011). Furthermore, the voltage-dependence of this persistent current was hyperpolarized by ~10 mV in $Na_v1.1$ cells treated with deltamethrin. Such a major shift in favor of more hyperpolarized potentials lying closer to Na_v voltage thresholds could explain the larger window currents for $Na_v1.1$ cells. $Na_v1.6$ cells treated with deltamethrin also showed an induction of persistent current, but the associated control values were not sigmoidal in nature and could not be fitted. We also observed that voltage-dependent tail current densities for both isoforms were potentiated with 10 μM deltamethrin application, but again, only $Na_v1.1$ retained a significant potentiation at 1 μM deltamethrin. Furthermore, $Na_v1.6$ tail current densities follow a relatively linear pattern in their current-voltage relationship that places the maximum current densities with the maximum voltage at +40 mV, but $Na_v1.1$ displays a shifted peak occurring at −10 mV that tapers and stabilizes with increasing voltage. It is uncertain what mechanism underlies this shift to −10 mV or the differences in shape, but this curve is similar to the tail currents induced by tefluthrin (a type I pyrethroid) as reported by

He and Soderlund (2011). Additionally, we were only able to detect significant changes in $Na_v1.6$ cells at 10 μM deltamethrin, which is markedly higher than the ~0.1 μM threshold identified in He and Soderlund (2015). This contradiction may be a result of the transient transfection used in (He and Soderlund, 2015) as opposed to our cell line that stably expresses a Na_v isoform, as the former yielded higher current magnitudes that could have allowed for more sensitive assays. Additionally, it should be noted that our experiments employed a static bath design, which differed from other studies that typically use perfusion-based methods. While this does limit our direct comparisons to results from other studies because of varying experimental designs, there are still several comparisons that can be inferred even among varying experimental conditions. Nonetheless, within the context of our experiments, $Na_v1.1$ is more sensitive to resting deltamethrin modification of persistent and tail currents than $Na_v1.6$.

In use-dependent protocols, neither isoform demonstrated a change in peak current density with deltamethrin treatment, but $Na_v1.6$ did show a significant increase in the degree of change induced by a train of depolarizations. This is consistent with previous studies demonstrating a use-dependent increase of $Na_v1.6$ function (Tan and Soderlund, 2010; He and Soderlund, 2011, 2015). Deltamethrin did produce significant increases to both persistent currents and tail currents in both isoforms, which is consistent with previous studies of $Na_v1.6$ (Tan and Soderlund, 2010, 2009; He and Soderlund, 2011). However, no value was accompanied with a significant% change from the initial test pulse in $Na_v1.1$ recordings, indicating that enhancement of persistent and tail currents occurred prior to recording during the incubation phase and is not use-dependent. Deltamethrin did produce a significant and use-dependent increase of the fraction of available current for both isoforms, indicating deltamethrin exposure results in an increased population of inactivation-resistant $Na_v1.1$ and $Na_v1.6$ channels, which is seen in other isoforms as well (Tan and Soderlund, 2010, 2009; He and Soderlund, 2011; McCavera and Soderlund, 2012). Due to the robust persistence of currents induced by deltamethrin exposure, the time constant of decay was not able to be determined. However, using the area under the curve to indicate total charge flux, we found that deltamethrin significantly increased the amount of Na^+ able to cross the membrane in a use-dependent manner, which is consistent with similar measures in other studies of Na_v channel isoforms (Tan and Soderlund, 2010, 2009; He and Soderlund, 2011; McCavera and Soderlund, 2012). We found the same effect in $Na_v1.6$, but the magnitude of charge was much lower. Taken together, these data indicate that $Na_v1.6$ channels are much more amenable to use-dependent alteration than their $Na_v1.1$ counterparts. $Na_v1.1$ channels do show significant changes in persistent and tail currents when compared to DMSO control, but when compared with naïve channel prior to depolarization trains there is no difference, indicating these changes could have occurred during incubation and are not likely use-dependent.

In conclusion, our results indicate that the $Na_v1.1$ α subunit isoform is vulnerable to deltamethrin exposure at concentrations equivalent to or lower than concentrations needed to effect similar changes in $Na_v1.6$, which was not predicted based on phylogenetic similarity to $Na_v1.2$ (Catterall et al., 2005; Oliveira et al., 2013) and the presence of an isoleucine at the 409 (cockroach) residue (O'Reilly et al., 2006; Oliveira et al., 2013; Tan et al., 2005; Du et al., 2011). Similar to other isoforms, deltamethrin effected use-dependent enhancement of

the fraction of available current and total charge flux in both $Na_v1.1$ and $Na_v1.6$ (Tan and Soderlund, 2010, 2009; He and Soderlund, 2011; McCavera and Soderlund, 2012). Persistent and tail currents were potentiated with deltamethrin exposure at a lower concentration than needed for similar effects in $Na_v1.6$, but repeated depolarizing trains only enhanced $Na_v1.6$ modification, which indicates most channel modification of Nav1.1 occurs at rest without use-dependent enhancement. It is possible that the addition of Na_v β subunits could alter the behavior of these channels and possibly confer use-dependence on one or both of the channels, bringing them in line with other studies (Tan and Soderlund, 2010; He and Soderlund, 2011, 2015). A previous study (He and Soderlund, 2011) indicated that deltamethrin, a type II pyrethroid, enhances tail currents and delays the onset of inactivation in a use-dependent manner while tefluthrin, a type I pyrethroid, induced more resting-state modification than deltamethrin. Considering that deltamethrin demonstrates some characteristics of type I pyrethroids, as indicated in (Breckenridge et al., 2009), the resting-state bias for $Na_v1.1$ observed in this study may be a result of this overlap of characteristics. Therefore, various Na_v isoforms may be biased toward either resting-state or open-state modification depending on where the pyrethroid falls in the continuum between type I and type II characteristics, and as a result, they favor one type of pyrethroid over the other. If correct, this hypothesis suggests that a pyrethroid associated primarily with type I characteristics, like permethrin (Breckenridge et al., 2009), would induce resting modification of $Na_v1.1$ while a pyrethroid that primarily demonstrates type II characteristics, such as λ-cyhalothrin (Breckenridge et al., 2009) would effect little to no use-dependent modification. Conversely, $Na_v1.6$ should be comparatively more amenable to modification by a type II pyrethroid like λ-cyhalothrin rather than a type I pyrethroid such as permethrin. Taken together, our data show that $Na_v1.1$ is susceptible to deltamethrin modification at lower concentrations than for $Na_v1.6$, but this susceptibility stems from a bias toward resting modification over use-dependent, demonstrating that Na_v isoforms have differential responses to the same pyrethroid treatment. With significant susceptibility to deltamethrin, Nav1.1 might be the biological link between early-life exposure to pyrethroids, impaired function of inhibitory fast-spiking interneurons (where Nav1.1 is abundantly expressed) and increased risk for neurodevelopmental disorders in the human population (Viel et al., 2015; Richardson et al., 2015; Ogiwara et al., 2007; Berkowicz et al., 2016; Dong et al., 2016; Inan et al., 2016; Jiang et al., 2013; McNally et al., 2013; Catterall et al., 2008; Lee et al., 2015). Future studies profiling activity of a broader spectrum of pyrethroids against Nav1.1 channels might generate improved EPA guidelines to prevent early-life exposure toxicity of pesticides.

Acknowledgements

This work was supported by NIH/NIEHS-T32ES007254 (TJ), NIH/NIEHS-T32ES007254 (CT), NIEHS Center Grant P30 ES006676 (FL) and NIH/NIMH 0955995 (FL).

References

Berkowicz SR, Featherby TJ, Qu Z, Giousoh A, Borg NA, Heng JI, et al. Brinp1 (−/−) mice exhibit autism-like behaviour, altered memory, hyperactivity and increased parvalbumin-positive cortical interneuron density. Mol. Autism. 2016; 7:22. [PubMed: 27042284]

Breckenridge CB, Holden L, Sturgess N, Weiner M, Sheets L, Sargent D, et al. Evidence for a separate mechanism of toxicity for the Type I and the Type II pyrethroid insecticides. Neurotoxicology. 2009; 30(Suppl. 1):S17–31. [PubMed: 19766671]

Catterall WA, Goldin AL, Waxman SG. International Union of Pharmacology: XLVII. Nomenclature and structure-function relationships of voltage-gated sodium channels. Pharmacol. Rev. 2005; 57(4): 397–409. [PubMed: 16382098]

Catterall WA, Dib-Hajj S, Meisler MH, Pietrobon D. Inherited neuronal ion channelopathies: new windows on complex neurological diseases. J. Neurosci. 2008; 28(46):11768–11777. [PubMed: 19005038]

Catterall WA. From ionic currents to molecular review mechanisms: the structure and function of voltage-gated sodium channels. Neuron. 2000; 26:13–25. [PubMed: 10798388]

Chinn K, Narahashi T. Stabilization of sodium channel states by deltamethrin in mouse neuroblastoma cells. J. Physiol. 1986; 380:191–207. [PubMed: 2441036]

Corcellas C, Eljarrat E, Barcelo D. First report of pyrethroid bioaccumulation in wild river fish: a case study in Iberian river basins (Spain). Environ. Int. 2015; 75:110–116. [PubMed: 25461420]

Cusdin FS, Clare JJ, Jackson AP. Trafficking and cellular distribution of voltage-gated sodium channels. Traffic. 2008; 9(1):17–26. [PubMed: 17988224]

Dong, X-W., Priestley, T. Current Protocols in Pharmacology. John Wiley & Sons, Inc; 2003. Electrophysiological analysis of tetrodotoxin-resistant sodium channel pharmacology; p. 11.8.1-8.33.

Dong F, Jiang J, McSweeney C, Zou D, Liu L, Mao Y. Deletion of CTNNB1 in inhibitory circuitry contributes to autism-associated behavioral defects. Hum. Mol. Genet. 2016; 25(13):2738–2751. [PubMed: 27131348]

Du Y, Khambay B, Dong K. An important role of a pyrethroid-sensing residue F1519 in the action of the N-alkylamide insecticide BTG 502 on the cockroach sodium channel. Insect Biochem. Mol. Biol. 2011; 41(7):446–450. [PubMed: 21426938]

Goldin AL. Resurgence of sodium channel research. Annu. Rev. Physiol. 2001; 63:871–891. [PubMed: 11181979]

Hartshorne RP, Catterall WA. The sodium channel in rat brain. J. Biol. Chem. 1984; 259:1667–1675. [PubMed: 6319405]

He B, Soderlund DM. Differential state-dependent modification of rat Na(v) 1.6 sodium channels expressed in human embryonic kidney (HEK293) cells by the pyrethroid insecticides tefluthrin and deltamethrin. Toxicol. Appl. Pharmacol. 2011; 257(3):377–387. [PubMed: 21983428]

He B, Soderlund DM. Effects of the beta1 auxiliary subunit on modification of Rat Na1.6 sodium channels expressed in HEK293 cells by the pyrethroid insecticides tefluthrin and deltamethrin. Toxicol. Appl. Pharmacol. 2015; 291:58–69. [PubMed: 26708501]

Inan M, Zhao M, Manuszak M, Karakaya C, Rajadhyaksha AM, Pickel VM, et al. Energy deficit in parvalbumin neurons leads to circuit dysfunction, impaired sensory gating and social disability. Neurobiol. Dis. 2016; 93:35–46. [PubMed: 27105708]

James TF, Nenov MN, Wildburger NC, Lichti C, Luisi J, Vergara F, et al. The $Na_V1.2$ channel is regulated by GSK3. Biochim. Biophys. Acta. 2015:832–844.

Jiang Z, Cowell RM, Nakazawa K. Convergence of genetic and environmental factors on parvalbumin-positive interneurons in schizophrenia. Front. Behav. Neurosci. 2013; 7:116. [PubMed: 24027504]

Lee I, Eriksson P, Fredriksson A, Buratovic S, Viberg H. Developmental neurotoxic effects of two pesticides: behavior and neuroprotein studies on endosulfan and cypermethrin. Toxicology. 2015; 335:1–10. [PubMed: 26143737]

Leterrier C, Brachet A, Fache MP, Dargent B. Voltage-gated sodium channel organization in neurons: protein interactions and trafficking pathways. Neurosci. Lett. 2010; 486(2):92–100. [PubMed: 20817077]

McCavera SJ, Soderlund DM. Differential state-dependent modification of inactivation-deficient Nav1.6 sodium channels by the pyrethroid insecticides S-bioallethrin, tefluthrin and deltamethrin. Neurotoxicology. 2012; 33(3):384–390. [PubMed: 22465659]

McNally JM, McCarley RW, Brown RE. Impaired GABAergic neurotransmission in schizophrenia underlies impairments in cortical gamma band oscillations. Curr. Psychiatry Rep. 2013; 15(3):346. [PubMed: 23400808]

Motomura H, Narahashi T. Interaction of tetramethrin and deltamethrin at the single sodium channel in rat hippocampal neurons. Neurotoxicology. 2001; 32:9–39.

Mowry JB, Spyker DA, Cantilena LR Jr. McMillan N, Ford M. 2013 Annual report of the american association of poison control centers' national poison data system (NPDS): 31st annual report. Clin. Toxicol. (Phila.). 2014; 52(10):1032–1283. [PubMed: 25559822]

O'Reilly AO, Khambay BP, Williamson MS, Field LM, Wallace BA, Davies TG. Modelling insecticide-binding sites in the voltage-gated sodium channel. Biochem. J. 2006; 396(2):255–263. [PubMed: 16475981]

Ogiwara I, Miyamoto H, Morita N, Atapour N, Mazaki E, Inoue I, et al. Nav1.1 localizes to axons of parvalbumin-positive inhibitory interneurons: a circuit basis for epileptic seizures in mice carrying an Scn1a gene mutation. J. Neurosci. 2007; 27(22):5903–5914. [PubMed: 17537961]

Oliveira EE, Du Y, Nomura Y, Dong K. A residue in the transmembrane segment 6 of domain I in insect and mammalian sodium channels regulate differential sensitivities to pyrethroid insecticides. Neurotoxicology. 2013; 38:42–50. [PubMed: 23764339]

Oulhote Y, Bouchard MF. Urinary metabolites of organophosphate and pyrethroid pesticides and behavioral problems in Canadian children. Environ. Health Perspect. 2013; 121(11–12):1378–1384. [PubMed: 24149046]

Power LE, Sudakin DL. Pyrethrin and pyrethroid exposures in the United States: a longitudinal analysis of incidents reported to poison centers. J. Med. Toxicol. 2007; 3(3):94–99. [PubMed: 18072143]

Qiao X, Sun G, Clare JJ, Werkman TR, Wadman WJ. Properties of human brain sodium channel alpha-subunits expressed in HEK293 cells and their modulation by carbamazepine, phenytoin and lamotrigine. Br. J. Pharmacol. 2014; 171(4):1054–1067. [PubMed: 24283699]

Ray DE, Fry JR. A reassessment of the neurotoxicity of pyrethroid insecticides. Pharmacol. Ther. 2006; 111(1):174–193. [PubMed: 16324748]

Richardson JR, Taylor MM, Shalat SL, Guillot TS 3rd, Caudle WM, Hossain MM, et al. Developmental pesticide exposure reproduces features of attention deficit hyperactivity disorder. FASEB J. 2015; 29(5):1960–1972. [PubMed: 25630971]

Romero A, Ares I, Ramos E, Castellano V, Martinez M, Martinez-Larranaga MR, et al. Evidence for dose-additive effects of a type II pyrethroid mixture. In vitro assessment. Environ. Res. 2015; 138:58–66. [PubMed: 25688004]

Shavkunov AS, Wildburger NC, Nenov MN, James TF, Buzhdygan TP, Panova-Elektronova NI, et al. The fibroblast growth factor 14: voltage-gated sodium channel complex is a new target of glycogen synthase kinase 3 (GSK3). J. Biol. Chem. 2013; 288(27):19370–19385. [PubMed: 23640885]

Tan J, Soderlund DM. Human and rat Nav1.3 voltage-gated sodium channels differ in inactivation properties and sensitivity to the pyrethroid insecticide tefluthrin. Neurotoxicology. 2009; 30(1):81–89. [PubMed: 19026681]

Tan J, Soderlund DM. Divergent actions of the pyrethroid insecticides S-bioallethrin, tefluthrin, and deltamethrin on rat Na(v)1.6 sodium channels. Toxicol. Appl. Pharmacol. 2010; 247(3):229–237. [PubMed: 20624410]

Tan J, Liu Z, Wang R, Huang ZY, Chen AC, Gurevitz M, et al. Identification of amino acid residues in the insect sodium channel critical for pyrethroid binding. Mol. Pharmacol. 2005; 67(2):513–522. [PubMed: 15525757]

Tatebayashi H, Narahashi T. Differential mechanism of action of the pyrethroid tetramethrin on tetrodotoxin-densitive and tetrodotoxin-resistant sodium channels. J. Pharmacol. Exp. Ther. 1994; 270(2):595–603. [PubMed: 8071852]

Vais H, Atkinson S, Eldursi N, Devonshire AL, Williamson MS, Usherwood PNR. A single amino acid change makes a rat neuronal sodium channel highly sensitive to pyrethroid insecticides. FEBS Lett. 2000; 470:135–138. [PubMed: 10734222]

Viel JF, Warembourg C, Le Maner-Idrissi G, Lacroix A, Limon G, Rouget F, et al. Pyrethroid insecticide exposure and cognitive developmental disabilities in children: the PELAGIE mother-child cohort. Environ. Int. 2015; 82:69–75. [PubMed: 26057254]

Wildburger NC, Ali SR, Hsu WC, Shavkunov AS, Nenov MN, Lichti CF, et al. Quantitative proteomics reveals protein–protein interactions with fibroblast growth factor 12 as a component of the voltage-gated sodium channel 1.2 (nav1.2) macromolecular complex in Mammalian brain. Mol. Cell. Proteomics. 2015; 14(5):1288–1300. [PubMed: 25724910]

Yarov-Yarovoy V, Brown J, Sharp EM, Clare JJ, Scheuer T, Catterall WA. Molecular determinants of voltage-dependent gating and binding of pore-blocking drugs in transmembrane segment IIIS6 of the Na(+) channel alpha subunit. J. Biol. Chem. 2001; 276(1):20–27. [PubMed: 11024055]

Yarov-Yarovoy V, McPhee JC, Idsvoog D, Pate C, Scheuer T, Catterall WA. Role of amino acid residues in transmembrane segments IS6 and IIS6 of the Na+ channel alpha subunit in voltage-dependent gating and drug block. J. Biol. Chem. 2002; 277(38):35393–35401. [PubMed: 12130650]

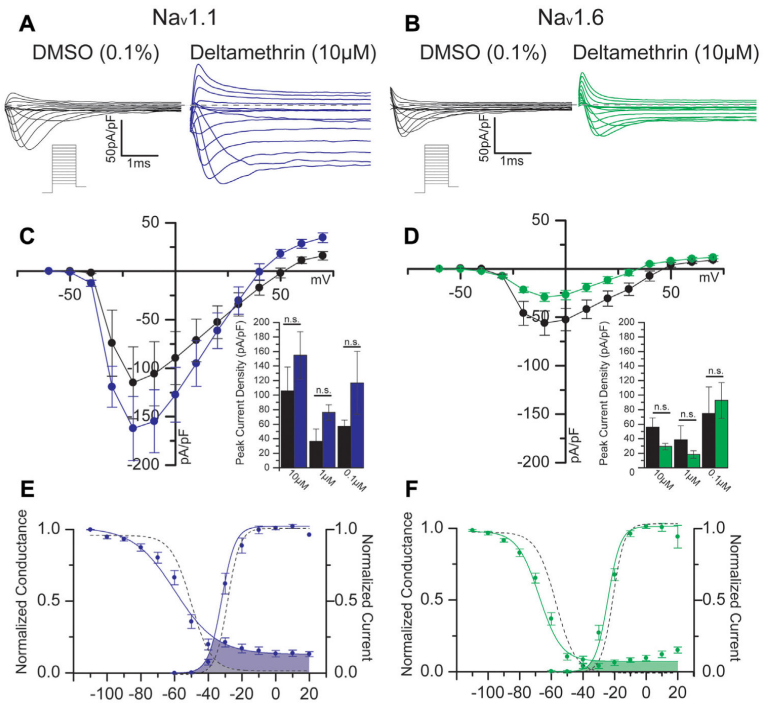

Fig. 1.

Representative traces of HEK-$Na_v1.1$ (**A**) or HEK-$Na_v1.6$ (**B**) cells in DMSO or deltamethrin-treated conditions in response to an evoked step-wise protocol (schematic under traces). With DMSO in black, Panels **C** and **D** depict a current-voltage relationship for $Na_v1.1$ and $Na_v1.6$, respectively, showing deltamethrin treatment in blue for $Na_v1.1$ and green for $Na_v1.6$. Summary bar graphs comparing peak current densities at −10 mV for all three concentrations are shown below the I–V graphs. Voltage-dependencies of activation and steady-state inactivation are depicted for $Na_v1.1$ (**E**) and $Na_v1.6$ (**F**); control curves are represented with dashed lines. Window currents are depicted where activation and steady-state inactivation curves overlap, which is indicated with shaded areas—gray for DMSO and colors for deltamethrin. Error bars indicate SEM. (For interpretation of the references to colour in this figure legend, the reader is referred to the web version of this article.)

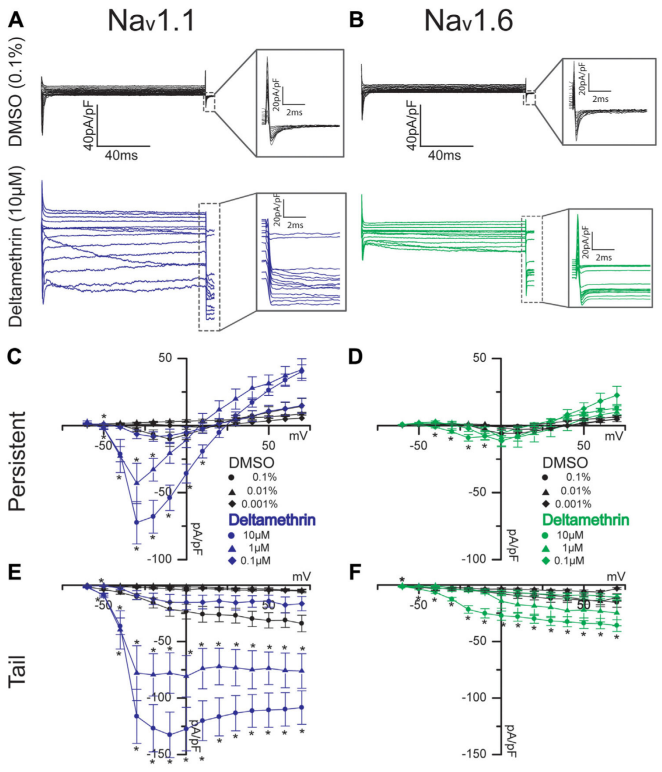

Fig. 2.

Representative traces of persistent currents and tail currents (insets) are shown for HEK-$Na_v1.1$ cells (**A**) and HEK-$Na_v1.6$ cells (**B**) with deltamethrin shown in blue and green, respectively. Current-voltage relationships are shown for $Na_v1.1$ and $Na_v1.6$ persistent currents (**C, D**, respectively) and for $Na_v1.1$ and $Na_v1.6$ tail currents (**E, F**, respectively). Circles represent 10 μM or 0.1% final DMSO concentration; triangles represent 1 μM or 0.01% final DMSO concentration, and diamonds indicate 0.1 μM or 0.001% final DMSO concentration. Error bars indicate SEM. (For interpretation of the references to colour in this figure legend, the reader is referred to the web version of this article.)

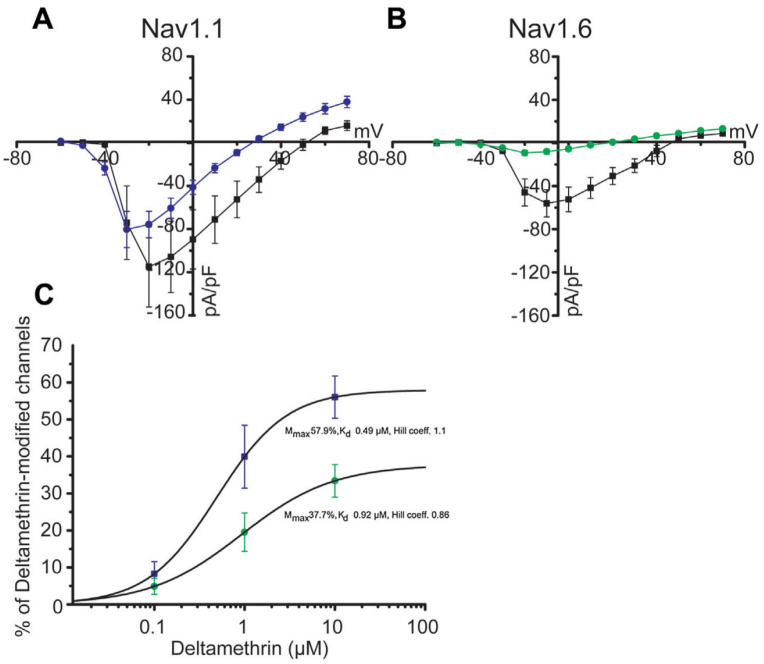

Fig. 3.

Current-voltage relationship for $Na_v1.1$ (A) and $Na_v1.6$ (B) depicting DMSO control peak currents (black squares) and deltamethrin persistent currents (colored circles). Concentration-dependent effect of deltamethrin as percentage of deltamethrin modified channels shown in C, with $Na_v1.1$ represented in blue and $Na_v1.6$ in green. Error bars indicate SEM. (For interpretation of the references to colour in this figure legend, the reader is referred to the web version of this article.)

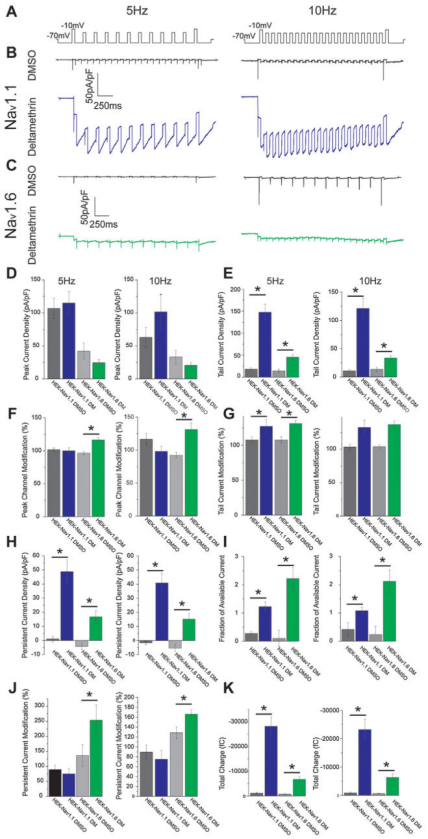

Fig. 4.

Representative traces of: **A**) Use-dependent stimulation protocols, **B**) HEK-$Na_v1.1$ cells treated with DMSO (black) or 10 μM deltamethrin (blue), **C**) HEK-$Na_v1.6$ cells treated with DMSO (black) or 10 μM deltamethrin (green). Below traces are summary bar graphs for both stimulation frequencies representing: **D**) Peak current density, **E**) Tail current density, **F**) Peak current density modification, **G**) Tail current density modification, **H**) Persistent current density, **I**) Fraction of available current, **J**) Peak current modification, **K**) Total charge. Error bars indicate SEM. (For interpretation of the references to colour in this figure legend, the reader is referred to the web version of this article.)

Table 1

Evoked Properties.

Isoform	**$Na_v1.1$**		**$Na_v1.6$**	
Treatment	**DMSO (0.1%)**	**Deltamethrin (10μM)**	**DMSO (0.1%)**	**Deltamethrin (10μM)**
Peak Current Density[a] (pA/pF)	105.9 ± 33.0 (9)	154.7 ± 32.4 (19)	56.1 ± 12.6 (10)	29.3 ± 4.4 (20)
Persistent Current Density[b] (pA/pF)	6.8 ± 3.6 (4)	68.0 ± 12.2 * (19)	−0.4 ± 0.6 (6)	9.2 ± 2.4 * (20)
Tail Current Density[a] (pA/pF)	21.4 ± 6.3 (9)	118.6 ± 18.5 * (14)	5.9 ± 1.5 (10)	25.1 ± 4.1 * (20)
Activation ($V_{1/2}$)	−22.6 ± 2.7 (7)	−27.2 ± 6.7 (12)	−20.7 ± 1.3 (10)	−23.8 ± 1.3 (17)
Activation Slope Factor (k)	2.9 ± 0.42 (7)	3.9 ± 0.60 (12)	3.6 ± 0.3 (10)	5.0 ± 0.3 * (17)
Persistent Activation ($V_{1/2}$)	−22.8 ± 1.4 (4)	−34.7 ± 1.1 * (16)	N/A	−26.8 ± 1.4 (9)
Persistent Activation Slope Factor (k)	6.5 ± 0.9 (4)	2.8 ± 0.3 * (16)	N/A	4.7 ± 1.1 (9)
Inactivation ($V_{1/2}$)	−50.4 ± 5.0 (8)	−53.9 ± 4.7 (13)	−56.6 ± 0.8 (12)	−64.5 ± 1.3 * (15)
Inactivation Slope Factor (k)	5.9 ± 0.7 (8)	5.2 ± 0.4 (13)	5.9 ± 0.2(12)	5.8 ± 0.3 (15)

Data are presented as Mean ± SEM.

* $p < 0.05$, n in parenthesis.

[a] Peaks taken at −10mV.

[b] Peaks taken at − 20 mV.

Table 2

Use-dependent Properties.

Parameter	HEK-$Na_v1.1$				HEK-$Na_v1.6$			
	DMSO (0.1%)		Deltamethrin (10μM)		DMSO (0.1%)		Deltamethrin (10μM)	
Stimulation Frequency (Hz)	10	5	10	5	10	5	10	5
Peak Current Density (pA/pF)	63.2 ± 15.0 (10)	101.6 ± 26.6 (10)	100.0 ± 17.8 (17)	121.8 ± 24.2 (17)	33.3 ± 10.2 (11)	42.1 ± 12.5 (11)	21.4 ± 3.6 (19)	25.5 ± 4.3 (19)
% Peak Current Density	116.4 ± 9.0 (10)	101.6 ± 2.8 (10)	98.1 ± 7.1 (17)	99.9 ± 4.4 (17)	92.2 ± 4.4 (11)	96.5 ± 2.4 (11)	119.0 ± 7.0 * (19)	120.6 ± 8.0 * (19)
Persistent Current Density (pA/pF)	−1.6 ± 1.3 (10)	1.1 ± 2.0 (10)	54.9 ± 9.1 * (17)	60.5 ± 7.6 * (17)	-4.6 ± 2.2 (12)	−3.5 ± 1.8 (12)	26.0 ± 7.0 * (19)	11.8 ± 2.5 (19)
% Persistent Current Density	89.6 ± 14.7 (10)	67.4 ± 27.4 (10)	75.1 ± 17.8 (12)	83.6 ± 10.7 (12)	119.6 ± 14.1 (11)	136.7 ± 36.0 (11)	276.8 ± 49.8 * (19)	253.8 ± 50.8 * (18)
Tail Current Density (pA/pF)	10.9 ± 2.1 (10)	17.9 ± 3.4 (10)	121.1 ± 18.2 (17)	147.8 ± 18.1 * (17)	13.4 ± 3.9 (12)	14.3 ± 3.6 (12)	33.4 ± 4.2 * (20)	45.5 ± 5.7 * (20)
% Tail Current Density	103.4 ± 4.0 (10)	107.7 ± 4.4 (10)	132.7 ± 10.8 (17)	127.1 ± 9.8 (17)	103.9 ± 2.9 (12)	107.8 ± 4.6 (12)	137.1 ± 4.8 * (20)	131.0 ± 5.1 (20)
Fraction of Available Current	0.42 ± 0.24 (9)	0.27 ± 0.06 (9)	1.23 ± 0.11 * (17)	1.49 ± 0.16 (17)	0.23 ± 0.29 (11)	0.10 ± 0.28 (11)	2.07 ± 0.28 * (19)	2.12 ± 0.26 * (19)
Total Charge (Q)	880.0 ± 292.4 (10)	1087.4 ± 389.2 (10)	23247.9 ± 3679.6 * (17)	28143.5 ± 3745.8 * (17)	624.1 ± 108.7 (12)	747.3 ± 218.5 (12)	5522.2 ± 780.1 * (20)	6080.3 ± 805.0 * (20)

Data are presented as Mean ± SEM.

* $p<0.05$.